

# Energy Transfer, Excited-State Deactivation, and Exciplex Formation in Artificial Caroteno-Phthalocyanine Light-Harvesting Antennas<sup>†</sup>

Rudi Berera,<sup>‡</sup> Ivo H. M. van Stokkum,<sup>‡</sup> Gerdenis Kodis,<sup>§</sup> Amy E. Keirstead,<sup>§</sup> Smitha Pillai,<sup>§</sup> Christian Herrero,<sup>§</sup> Rodrigo E. Palacios,<sup>§</sup> Mikas Vengris,<sup>‡</sup> Rienk van Grondelle,<sup>‡</sup> Devens Gust,<sup>\*,§</sup> Thomas A. Moore,<sup>\*,§</sup> Ana L. Moore,<sup>\*,§</sup> and John T. M. Kennis<sup>\*,‡</sup>

Department of Biophysics, Division of Physics and Astronomy, Faculty of Sciences, Vrije Universiteit, Amsterdam 1081 HV, The Netherlands, and Department of Chemistry and Biochemistry and the Center for the Study of Early Events in Photosynthesis, Arizona State University, Tempe, Arizona 85287-1604

Received: February 5, 2007; In Final Form: March 20, 2007

We present results from transient absorption spectroscopy on a series of artificial light-harvesting dyads made up of a zinc phthalocyanine (Pc) covalently linked to carotenoids with 9, 10, or 11 conjugated carbon–carbon double bonds, referred to as dyads **1**, **2**, and **3**, respectively. We assessed the energy transfer and excited-state deactivation pathways following excitation of the strongly allowed carotenoid S<sub>2</sub> state as a function of the conjugation length. The S<sub>2</sub> state rapidly relaxes to the S\* and S<sub>1</sub> states. In all systems we detected a new pathway of energy deactivation within the carotenoid manifold in which the S\* state acts as an intermediate state in the S<sub>2</sub> → S<sub>1</sub> internal conversion pathway on a sub-picosecond time scale. In dyad **3**, a novel type of collective carotenoid–Pc electronic state is observed that may correspond to a carotenoid excited state(s)–Pc Q exciplex. The exciplex is only observed upon direct carotenoid excitation and is nonfluorescent. In dyad **1**, two carotenoid singlet excited states, S<sub>2</sub> and S<sub>1</sub>, contribute to singlet–singlet energy transfer to Pc, making the process very efficient (>90%) while for dyads **2** and **3** the S<sub>1</sub> energy transfer channel is precluded and only S<sub>2</sub> is capable of transferring energy to Pc. In the latter two systems, the lifetime of the first singlet excited state of Pc is dramatically shortened compared to the 9 double-bond dyad and model Pc, indicating that the carotenoid acts as a strong quencher of the phthalocyanine excited-state energy.

## Introduction

Carotenoids are ubiquitous pigments in nature where they serve a number of functions. In photosynthetic systems they act mainly as light harvesters and photoprotectors.<sup>1</sup> They absorb light in the blue-green region of the spectrum and transfer the energy to neighboring chlorophylls.<sup>2</sup> In this spectral region chlorophylls display very little absorption; photosynthesis thus relies on carotenoids to optimize the absorption cross-section. Concerning the photoprotective role, carotenoids can scavenge injurious singlet oxygen and limit its sensitization by quenching chlorophyll triplet states.<sup>1</sup> Carotenoids are also involved in the thermal dissipation of excess energy in photosystem II (PSII) via the process of nonphotochemical quenching, and there is evidence that they can directly quench the singlet excited state of chlorophylls via either energy or electron transfer.<sup>3,4</sup>

All the aforementioned properties originate from the extraordinary excited-state manifold of carotenoids. The strong absorption in the visible region is due to the strongly allowed S<sub>0</sub> → S<sub>2</sub> transition. Hidden below the S<sub>2</sub> state is another singlet state, electronic dipole forbidden and known as S<sub>1</sub>.<sup>5–7</sup> In recent years it has become clear that this two excited-state levels representation is incomplete: additional electronic states that lie below S<sub>2</sub> have been theoretically predicted;<sup>5</sup> experimental evidence for some of them has been presented by several workers.<sup>8–12</sup>

The S\* state was discovered some years ago in spirilloxanthin, both in solution and bound to the light-harvesting (LH1) complex of *Rhodospirillum rubrum*.<sup>9</sup> It is characterized by an excited-state absorption (ESA) band blue-shifted with respect to that of the S<sub>1</sub> → S<sub>n</sub> absorption but red-shifted with respect to the optically allowed S<sub>0</sub> → S<sub>2</sub> transition. In spirilloxanthin bound to LH1, the S\* state is a precursor for the formation of the carotenoid triplet state on the picosecond time scale via the singlet fission mechanism. In later work, S\* was found in various carotenoids bound to light-harvesting (LH) complexes of other species of purple bacteria,<sup>11,13,14</sup> in some carotenoids in solution,<sup>15</sup> and in artificial LH constructs.<sup>16</sup> S\* is involved in energy transfer from carotenoid to chlorophyll (Chl) or other tetrapyrroles in many of these systems. In all cases, S\* and S<sub>1</sub> were formed in parallel by internal conversion (IC) from S<sub>2</sub> and evolved independently, decaying on the picosecond time scale by either IC, energy transfer, or, in the case of S\*, triplet formation. Despite its common occurrence, the electronic nature of S\* has remained rather elusive. It was proposed that it corresponds to the theoretically predicted, optically dark, <sup>1</sup>B<sub>u</sub><sup>−</sup> state<sup>9</sup> or to excited dark states in geometrically distorted carotenoids.<sup>17</sup> Alternatively, it was suggested that S\* corresponds to a hot ground state.<sup>18</sup>

In recent years advances in chemical synthesis have made it possible to synthesize artificial light-harvesting antennas capable of mimicking many of the functions carried out by their natural counterparts.<sup>16,19,20</sup> These systems mimic light-harvesting, energy transfer, electron transfer, and photoprotective functions of natural photosynthesis. The study of model systems is of increasing interest for several reasons: the simplicity of the

<sup>†</sup> Part of the special issue “Norman Sutin Festschrift”.

\* Authors to whom correspondence should be addressed. E-mail: gust@asu.edu; tmoore@asu.edu; amooore@asu.edu; john@nat.vu.nl.

<sup>‡</sup> Vrije Universiteit.

<sup>§</sup> Arizona State University.

systems, typically made up of a very small number of chromophores, allows one to establish the basic photophysical and photochemical mechanisms underlying the behavior of the natural systems. Of more practical interest would be the incorporation of these systems into nanodevices, where they could function in light-harvesting, photoprotection, and energy transduction.

In this report we describe our studies of the photophysics of a series of three dyads made up of a zinc phthalocyanine (Pc) covalently linked to a carotenoid with 9, 10, or 11 conjugated double bonds. We determined the energy transfer and energy deactivation pathways following excitation of the carotenoid moiety to its strongly allowed  $S_2$  state. We report a previously unobserved pathway of energy deactivation within the carotenoid, where the  $S^*$  state acts as an intermediate in the  $S_2 \rightarrow S_1$  IC pathway. In dyad **3**, a novel type of collective carotenoid–Pc electronic state is observed that may correspond to a carotenoid excited state(s)–Pc Q exciplex. In dyad **1** a multiphasic carotenoid to Pc energy transfer process is observed, assigned to contributions from the carotenoid  $S_2$  and  $S_1$  excited states as well as a minor contribution from the hot  $S_1$ – $S^*$  excited state. As the conjugation length of the carotenoid is increased to 10 and 11 double bonds in dyad **2** and dyad **3**, respectively, the hot  $S_1$  and  $S_1$  energy transfer deactivation channels are precluded.

## Materials and Methods

The synthesis of the compounds has been previously described.<sup>4</sup> Femtosecond transient absorption spectroscopy was carried out with a setup described in detail earlier.<sup>21</sup> The output of a 1 kHz amplified Ti:sapphire laser system (Coherent-BMI  $\alpha$ 1000) was used to drive a home-built non-collinear optical parametric amplifier. The excitation wavelength was tuned to 475 nm to selectively excite the  $S_2$  state of the carotenoid moiety. The pulse width was 100 fs, and the energy was 100 nJ per pulse. A white light continuum, generated by focusing amplified 800 nm light on a 1 mm  $\text{CaF}_2$  crystal, served as a probe beam. The pump and probe were focused on a 1 mm path length cuvette, and to avoid sample degradation and exposure of the sample to multiple laser shots, the cuvette was mounted on a shaker. The polarization between pump and probe was set to the magic angle (54.7°).

The data were first analyzed globally using a sequential model with increasing lifetimes.<sup>22</sup> The data are thus described by a small number of lifetimes and evolution-associated difference spectra (EADS). Each EADS corresponds in general to a mixture of states and does not portray the spectrum of a pure state. To extract spectra of pure states a target analysis model was also applied to our data.<sup>22</sup>

The fluorescence up-conversion measurement was carried out by employing laser pulses of 100 fs at 800 nm generated from an amplified, mode-locked Ti:sapphire kilohertz laser system (Millennia/Tsunami/Spitfire, Spectra Physics). Part of the laser pulse energy (gate pulse) was sent through an optical delay line and mixed with the sample fluorescence in a 1 mm  $\beta$ -barium borate (BBO) crystal. The remainder of the pulse energy was used to pump an optical parametric amplifier (Spectra Physics) to generate excitation pulses. Up-converted UV light was sent through a double monochromator and recorded by a photomultiplier tube (PMT) coupled to a box car integrator (SR250, Stanford Research Systems). The absorption spectra were measured before and after each experiment to confirm sample stability.

## Results and Discussion

Figure 1A shows the structures of the compounds. The absorption spectra of dyads **1**, **2**, and **3** as well as model Pc **4** dissolved in tetrahydrofuran (THF) are shown in Figure 1B. Transient absorption experiments were performed on dyads **1**, **2**, and **3** with excitation of the carotenoid moiety at 475 nm and broadband detection with a white light continuum.

**Dyad 2.** Because dyad **2** exhibits the simplest behavior of the three systems studied, it will be discussed first. Figure 2A shows the EADS for dyad **2** in THF, whereas Figures 2B–D show kinetic traces at selected wavelengths. Nearly identical results were obtained for dyad **2** in dioxane as shown in Figure 1 of the Supporting Information. (For spectroscopic studies in different solvents see ref 4.) Five components are needed to satisfactorily fit the data. The first EADS (black line) appears at time zero and represents population of the optically allowed  $S_2$  state of the carotenoid. It presents a region of negative signal at wavelengths below 570 nm originating from the carotenoid ground-state bleach, stimulated emission in the 570–600 nm region, and a band-shift-like signal in the Pc Q region around 680 nm due to perturbation of Pc by the proximate excited carotenoid.

The first EADS decays in 58 fs into the second EADS (red line). This EADS presents the carotenoid ground-state bleach below 520 nm and carotenoid ESA between 520 and 650 nm. This ESA originates from both the  $S^*$  state, absorbing mainly in the 550 nm region, and the  $S_1$  state (around 570 nm) of the carotenoid populated from  $S_2$  via IC. In the region around 680 nm the ground-state bleach of the Pc Q-band is observed as well as a vibronic band at 610 nm. These bleaches on this time scale are *prima facie* evidence for carotenoid  $S_2$  to Pc energy transfer. The signal above 700 nm is due to carotenoid ESA.

The second EADS evolves into the third EADS (green line) in 840 fs. As before, in the region below 510 nm the carotenoid ground-state bleach is seen. The carotenoid excited-state region shows an interesting phenomenon: the signal below 555 nm has decreased concomitantly with an increase of the signal above this wavelength. This behavior is suggestive of an IC process within the carotenoid where the  $S_1$  state (ESA to the red of that of  $S^*$ ) is populated from the  $S^*$  state and was further investigated by target analysis (*vide infra*). Figures 2B and 2C show the kinetic traces for dyad **2** recorded at 550 and 570 nm, respectively, along with the corresponding fits from global analysis. The 550 nm data represent the decay of the  $S^* \rightarrow S_n$  ESA, and the 570 nm data represent the evolution of the  $S_1 \rightarrow S_n$  ESA. Within the first picosecond the two traces clearly show different dynamics in that the decrease in amplitude for the 550 nm trace (Figure 2B) is accompanied by an increase of the amplitude at 570 nm, further confirming the  $S^* \rightarrow S_1$  IC process. The fact that the Pc Q bleach at 680 nm (Figure 2D) does not increase with the decay of  $S^*$  (Figure 2B) or  $S_1$  (Figure 2C) supports the conclusion that neither the  $S^*$  state nor the  $S_1$  state is transferring energy to Pc in this system. Furthermore, energy transfer from  $S^*$  would repopulate the carotenoid ground state, and that is not observed. The ground-state bleach below 510 nm is similar in the second and third EADS.

The fourth EADS (blue line) appears after 8.1 ps. The structured carotenoid ESA above 510 nm has disappeared as well as the carotenoid ground-state bleach below 500 nm implying that the carotenoid  $S_1$  state has now decayed to the ground state. In the 520 nm region the spectrum presents a band-shift-like signal that is absent in the spectrum of the relaxed, fully solvated model Pc excited state (not shown) but previously

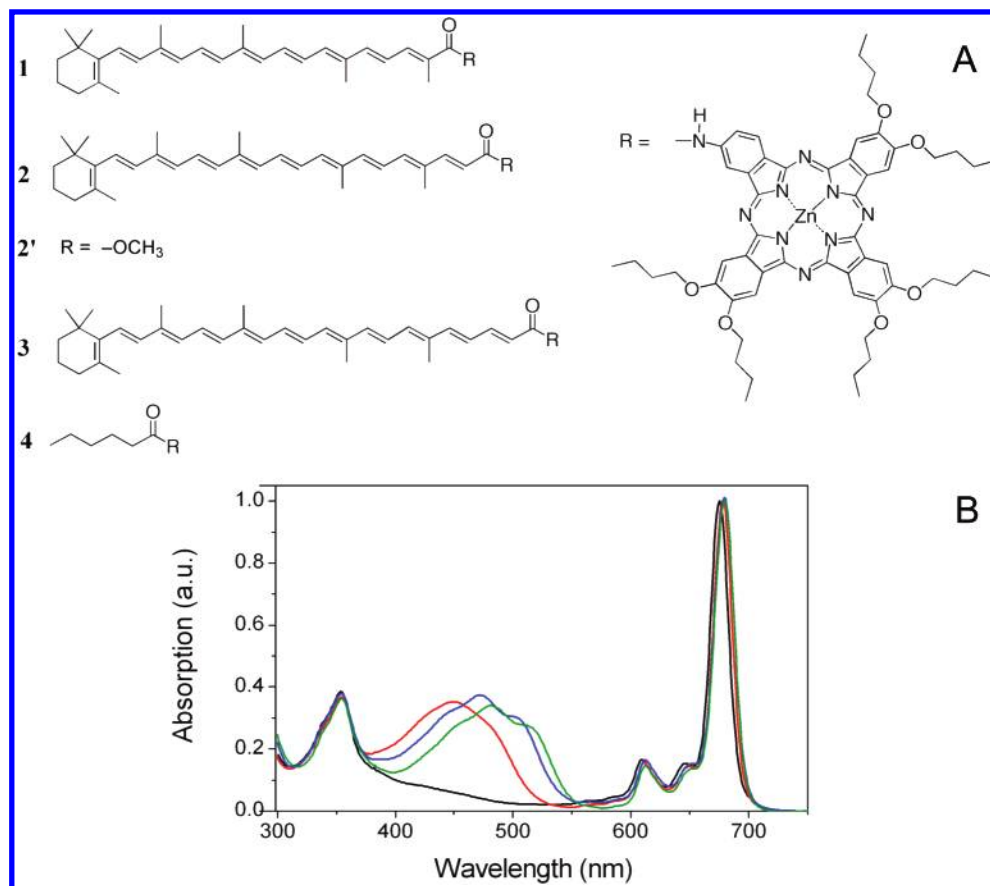


**Figure 1.** (A) Molecular structures of the dyads and reference carotenoid. A zinc phthalocyanine is covalently linked to a carotenoid with 9 conjugated carbon–carbon double bonds (dyad **1**), 10 carbon–carbon double bonds (dyad **2**), and 11 carbon–carbon double bonds (dyad **3**). Model carotenoid **2'** has a terminal methyl ester group instead of a phthalocyanine. (B) Absorption spectra in THF for dyads **1** (red line), **2** (blue line), and **3** (green line) and model Pc **4** (black line).

observed in the same dyad with excitation in the Pc Q state.<sup>4</sup> Similar phenomena were observed in photosynthetic light-harvesting complexes and assigned to a change of the local electric field of the carotenoid and excitonic coupling between Chl and the optically allowed carotenoid  $S_2$  state.<sup>23,24</sup> In the Pc bleach region (680 nm) there is no detectable increase of the bleach, indicating that the carotenoid  $S_1$  state is incapable of energy transfer to Pc.

A comparison of the  $S_1$  lifetime (8.1 ps) for dyad **2** with the  $S_1$  lifetime (12 ps) of the model carotenoid **2'**<sup>4,16</sup> reveals that the lifetime of the carotenoid (Car)  $S_1$  state in the dyad is shorter. In light of the absence of any energy transfer from the  $S_1$  state, this observation suggests that specific Car–Pc interactions lead to a shortening of the  $S_1$  lifetime in the dyad. Possibly, the vibronic coupling between the carotenoid ground and the  $S_1$  state has been enhanced by covalent linkage of Pc, leading to an enhanced rate of IC to the ground state. Note that in recombinant light-harvesting complex II (LHCII) with altered carotenoid pigments a similar phenomenon was observed.<sup>25</sup>

The fifth EADS (cyan line) appears in 268 ps and does not decay on the time scale of the experiment. We observe that by now the Pc Q bleach has almost disappeared and at the same time a broad ESA between 480 and 570 nm with low amplitude has appeared. The shape of this non-decaying EADS is likely to be due to a mixture of long-living species, e.g., Pc and carotenoid triplets. It is interesting to note that the lifetime of the Pc Q state (268 ps) is dramatically shorter compared to the lifetime of the Pc Q state in dyad **1** and model Pc (**3** ns) meaning that the 10 double-bond carotenoid acts as an effective quencher of the Q state of Pc.<sup>4</sup> The low amplitude of the fifth EADS

also indicates that the yield of the triplet species is minuscule; the quenching process primarily yields the ground state.

**Target Analysis of Dyad 2: Characterization of a  $S^* \rightarrow S_1$  IC Process.** The sequential analysis of the data allows one to extract the intrinsic lifetimes of the processes, but the spectra portrayed by such an analysis are not in general pure spectra of molecular species but rather represent a mixture of the latter. To provide further evidence of the  $S^* \rightarrow S_1$  IC process in the systems, we applied a target analysis of the data collected on dyad **2**, employing a specific kinetic model. The model is depicted in Figure 3A and consists of five compartments. The first compartment corresponds to the carotenoid  $S_2$  state. It decays to the  $S^*$  state by a fraction  $\Phi_1$  and to the  $S_1$  state by a fraction  $\Phi_2$ . A fraction  $\Phi_3$  transfers energy to give the Pc excited state, Pc\*. The  $S^*$  state decays to the ground state with rate constant  $k_1$  and undergoes IC to the  $S_1$  state with rate constant  $k_2$ . The  $S_1$  state decays entirely to the ground state (GS) with a rate constant  $k_3$ . The fourth compartment corresponds to the excited Pc, Pc\*, which transfers energy back to the  $S_1$  state with a rate constant  $k_4$ , decays to the ground state with a rate constant  $k_5$ , and undergoes intersystem crossing (ISC) to the triplet state with a rate constant  $k_6$ .

The species-associated difference spectra (SADS) obtained from the target analysis are displayed in Figure 3B; the estimated rate constants and branching fractions are summarized in Table 1. The SADS corresponding to  $S_2$  is not shown. The  $S_2$  state decays to the  $S^*$  state (red SADS) with  $\Phi_1 = 15\%$  and to the  $S_1$  state (green SADS) with  $\Phi_2 = 25\%$  and by energy transfer to Pc with  $\Phi_3 = 60\%$ .  $S^*$  decays to the ground state with a rate constant  $k_1$  ( $4 \text{ ps}^{-1}$ ) and to the  $S_1$  state with a rate

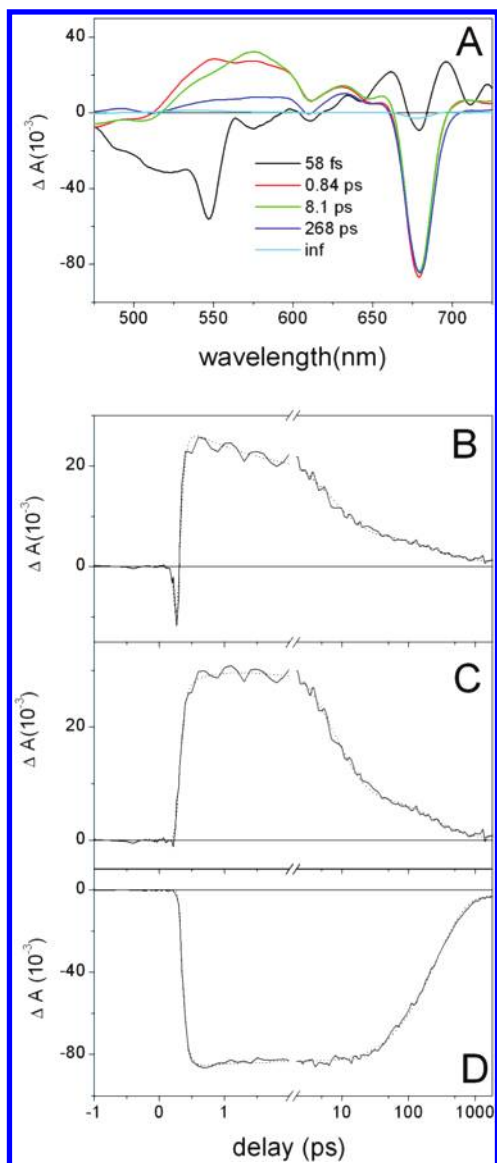


**Figure 2.** (A) Evolution-associated difference spectra that follow from a global analysis of data for dyad **2** in THF with excitation at 475 nm. (B) Kinetic trace with excitation at 475 nm and detection at 550 nm for **2** (solid line), along with the result of the global analysis fit (dotted line). (C) Same as panel B with detection at 570 nm. (D) Same as panel B with detection at 680 nm.

constant  $k_2$  ( $4 \text{ ps}^{-1}$ ). The  $S_1$  state decays to the ground state with a rate constant  $k_3$  ( $8.3 \text{ ps}^{-1}$ ). The Pc Q singlet excited state (blue SADS) transfers energy to the carotenoid with a rate constant  $k_4$  ( $416 \text{ ps}^{-1}$ ), decays to the ground state with a rate constant  $k_5 = (830 \text{ ps})^{-1}$ , and undergoes ISC to the triplet state (cyan line) with a rate constant  $k_6 = (2.5 \text{ ns})^{-1}$ .

The SADS representing  $S^*$  (red line) has the typical shape of the  $S^* \rightarrow S_n$  absorption for a 10 double-bond carotenoid<sup>11</sup> with a peak at 547 nm, a tail above 575 nm, and a ground-state bleach below 497 nm. The SADS representing  $S_1$  (green line) has the typical shape of the  $S_1 \rightarrow S_n$  absorption: it peaks at 577 nm and displays a tail above 610 nm. Below 522 nm it shows a ground-state bleach. A comparison of the shapes of the two SADS with the rather broad and flat shape of the second EADS of dyad **2** (Figure 2A) shows that the separation of the spectral features of the two states has been successful. The SADS corresponding to excited Pc,  $Pc^*$  (blue line), has the typical shape of Pc in the Q state<sup>4</sup> with bleaches at 680 and 610 nm, and a flat ESA below 600 nm. We conclude that the

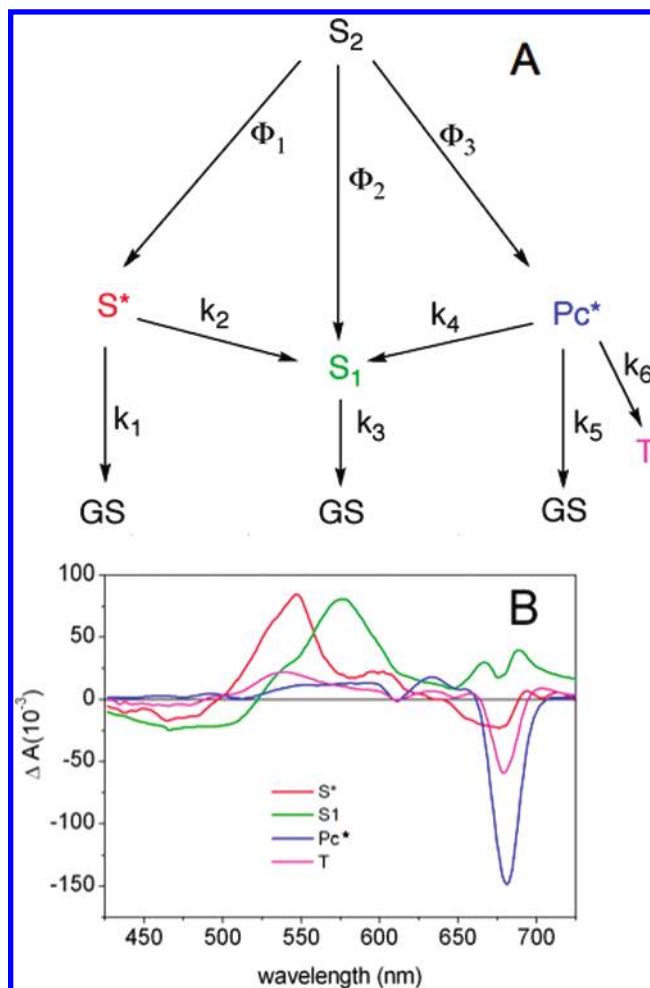


**Figure 3.** (A) Kinetic model used in the target analysis of the time-resolved data on dyad **2** (B) Species-associated difference spectra from the target analysis for dyad **2** in THF. See text for details.

target analysis adequately describes the spectral evolution of dyad **2** and provides good evidence that the  $S^*$  state undergoes IC to the  $S_1$  state.

**Dyad 3.** Figure 4A shows the EADS for dyad **3**, with kinetic traces shown in Figures 4B–D. Six components are needed for a good fit of the data as demonstrated by the strongly multiphasic character of the traces, especially in the 660–670 and 690–700 nm regions (see Figure 2 in the Supporting Information for a study in acetone). The first EADS (black line) appears at time zero and is associated with the carotenoid  $S_2$  state. It evolves into the second EADS (red line) in 43 fs. At this stage the  $S_2$  state has decayed to the  $S^*$  and  $S_1$  states as displayed by the broad ESA in the 525–620 nm region. Around 680 nm, the appearance of a large bleach signal is observed, corresponding partly to the Q state of Pc, indicating that energy transfer from the carotenoid  $S_2$  state to Pc has occurred (and partly population of a putative exciplex has taken place, vide infra).

The third EADS (green line) appears after 1.4 ps. This EADS shows a decrease of ESA corresponding to the  $S^*$  state and a concomitant increase of the signal in the 580–620 nm region. As for dyad **2**, we assign this evolution to the decay of the  $S^*$  state partly by IC to the ground state and partly by IC to the  $S_1$

**TABLE 1: Yields at Branching Points and Rate Constants for Dyad 2 in THF Obtained from Target Analysis**

$\Phi_1$	$\Phi_2$	$\Phi_3$	$k_1$	$k_2$	$k_3$	$k_4$	$k_5$	$k_6$
15%	25%	60%	$(4 \text{ ps})^{-1}$	$(4 \text{ ps})^{-1}$	$(8.3 \text{ ps})^{-1}$	$(416 \text{ ps})^{-1}$	$(830 \text{ ps})^{-1}$	$(2.5 \text{ ns})^{-1}$

state. Unlike the case with dyad **2**, the third EADS displays a decrease of the Pc Q bleach around 680 nm with respect to the second EADS. The evolution to the fourth EADS (blue line) takes place in 5.7 ps. It shows both carotenoid features with a bleach region below 540 nm and a considerably decreased carotenoid excited-state absorption in the 540 to 650 nm region. The decreased carotenoid ESA indicates that the carotenoid  $S_1$  state has decayed to the ground state. Concomitant with the decay of the  $S_1$  state, the fourth EADS features a further decrease of the Pc Q bleach.

The fifth EADS (cyan line) appears in  $\sim 18$  ps and has a lifetime of 90 ps. It displays Pc Q bleach in the 680 nm region and relatively flat excited-state absorption below 650 nm and

corresponds to the singlet excited state of Pc. The final EADS (magenta line) has a very low amplitude and corresponds to long-living triplet states. The lifetime of the Pc Q state, 90 ps, is shorter than that of Q in dyad **2**, and it is dramatically shortened compared to those of dyad **1** and model Pc, which implies that the carotenoid acts a strong quencher of the Q state of Pc, as noted previously.<sup>4</sup> Similar results were obtained for dyad **3** dissolved in acetone (Figure 2 in the Supporting Information).

A most intriguing observation of this experiment is that part of the carotenoid excited state(s) appears to decay together with the Pc Q state, mainly with a time constant of 18 ps. To investigate whether these decay processes are coupled, an experiment was carried out with excitation and detection in the Q state of Pc at 680 nm (Figure 4D, blue dash-dotted line). As can be seen from the kinetic traces in the 1–10 ps time frame, a picosecond decay component that is present upon excitation at 475 nm does not appear upon direct excitation of Pc at 680 nm. To further investigate this phenomenon a fluorescence up-conversion experiment was performed with selective excitation to the carotenoid  $S_2$  state at 480 nm and Pc fluorescence detection at 700 nm (Figure 4D, closed circles and red dashed line). The fluorescence kinetics do not show the fast decay component that is present in the transient absorption experiment upon carotenoid excitation.

We conclude that the concomitant decay of the carotenoid excited-state absorption and the Pc ground-state bleach is not fortuitous and must arise from a collective, nonfluorescent excited state containing both carotenoid and Pc character. A carotenoid excited state is the obligatory precursor of this state. Tentatively, this collective excited state can be assigned to an exciplex<sup>26</sup> formed by the carotenoid in the  $S_1$  and/or  $S^*$  state and Pc in the ground state. The occurrence of the putative exciplex and its spectral and temporal properties are investigated by applying a target analysis, as described below.

**Target Analysis of Dyad 3: Identification of a Carotenoid–Pc Exciplex.** For a better understanding of the photo-physics of dyad **3**, a target analysis has been applied with the kinetic model depicted in Figure 5A consisting of six compartments. The excited carotenoid  $S_2$  state decays in parallel to the  $S^*$  (fraction  $\Phi_1$ ) and  $S_1$  (fraction  $\Phi_2$ ) states as well as to a Car–Pc Q exciplex (denoted as EXC) with a fraction  $\Phi_3$ . The  $S_2$  state also transfers energy to the Pc moiety (fraction  $\Phi_4$ ). The  $S^*$  state besides decaying to the ground state with a rate constant  $k_3$  undergoes internal conversion to populate the  $S_1$  state (rate constant  $k_1$ ). The  $S_1$  state decays to the ground state with a rate constant  $k_2$ . The excited Pc is quenched by energy transfer to the carotenoid  $S_1$  state with a rate constant  $k_2$ , as observed earlier,<sup>4</sup> and partly decays to the long-living state denoted T, which corresponds to a mixture of Pc and carotenoid triplet states.

The SADS obtained from the kinetic model are displayed in Figure 5B, while the fractions and rate constants are reported in Table 2. The black SADS corresponds to the initially excited carotenoid  $S_2$  state. The red SADS corresponds to the  $S^*$  state with a ground-state bleach below 520 nm and excited-state absorption in the 520–600 nm region. Moreover, it shows a small negative signal in the Pc Q region. The SADS of the  $S_1$  state is in green and features carotenoid ground-state bleach below 540 nm and excited-state absorption between 540 and

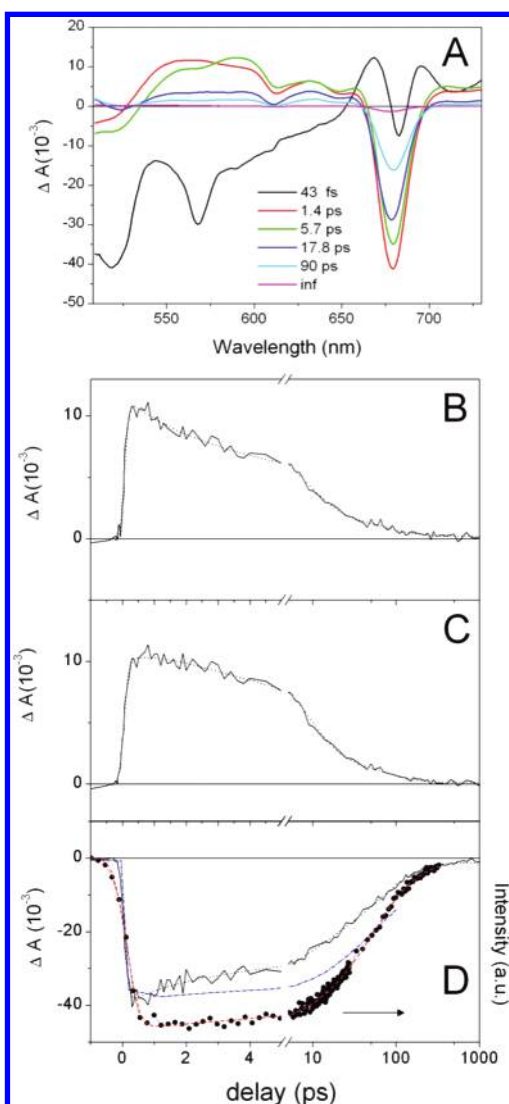


**Figure 4.** (A) Evolution-associated difference spectra that follow from a global analysis of data for dyad **3** in THF with excitation at 475 nm. (B) Kinetic trace with excitation at 475 nm and detection at 550 nm (solid line), along with the result of the global analysis fit (dotted line). (C) Same as panel B with detection at 590 nm. (D) Same as panel B with detection at 680 nm. The blue dash-dotted line denotes a kinetic trace with excitation and detection at 680 nm. Closed circles and the red dashed line show Pc fluorescence decay kinetics and a two exponential fit with 50 ps (80%, major component) and 220 ps lifetimes, respectively.

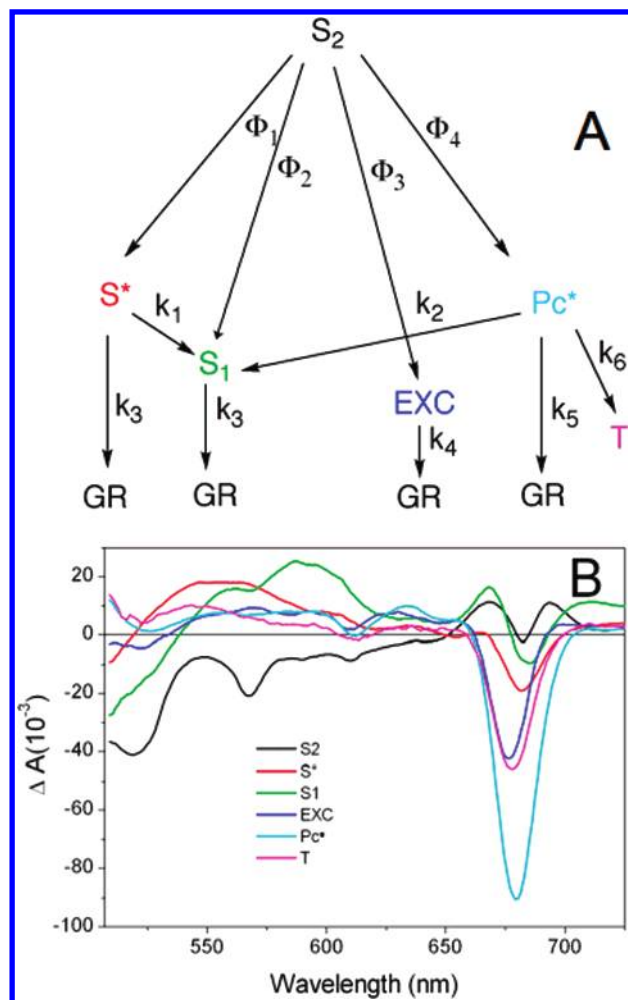


**Figure 5.** (A) Schematic representation of the excited-state energy transfer and IC pathways in dyad **3** upon excitation of the carotenoid moiety at 475 nm. EXC denotes an exciplex state between the carotenoid excited state(s) and the Pc Q state. See text for details. (B) Species-associated difference spectra from the target analysis for dyad **3** in THF. See text for details.

640 nm. In the Pc absorption region the spectrum shows a band-shift-like signal. The Pc excited state (cyan line) displays a bleach around 680 nm as well as a region of relatively flat excited-state absorption. The long-lived component (magenta line) corresponds to a mixture of carotenoid and Pc triplet states with the typical carotenoid  $T_1 \rightarrow T_n$  excited-state absorption in the 480–560 nm region and Pc Q bleach around 680 nm.

The blue SADS corresponds to the putative carotenoid–Pc exciplex. It displays carotenoid bleach below 530 nm and carotenoid excited-state absorption between 530 and ~730 nm. In the Pc Q region the spectrum displays bleaches. Thus, a mixture of Pc and carotenoid signals constitutes the SADS of the exciplex, consistent with the assignment to a carotenoid excited state–Pc Q exciplex. It is interesting to note that the exciplex bleach in the Pc Q region is blue-shifted with respect to the negative signal that results from the Pc singlet excited state (cf. cyan line). This observation indicates that stimulated emission from Pc does not contribute to the spectral shape and amplitude of the exciplex, consistent with our finding that the exciplex is non-emissive.

The occurrence of the exciplex upon relaxation from the  $S_2$  state may arise from excitonic interaction between the Pc Q states and the intense  $S_1/S^* \rightarrow S_n$  absorption of the carotenoid. Indeed, the  $S_1/S^* \rightarrow S_n$  absorption of the 11 double-bond carotenoid of dyad **3** is nearly in resonance with the vibronic band of the Pc Q transition near 610 nm, as can be observed in the third EADS in Figure 4A. (The vibronic Q bleach at 610 nm is nearly superimposed on the  $S_1/S^* \rightarrow S_n$  ESA.) In dyads **1** and **2**, the spectral overlap of the carotenoid  $S_1 \rightarrow S_n$  absorption with the vibronic Q-band is less extensive, which qualitatively explains the absence of such an exciplex in these systems. Moreover, the long carotenoid of dyad **3** (11 double bonds) is expected to be more flexible than the carotenoids of dyads **1** and **2**, which may lead to specific conformational changes of the carotenoid, as detected for caroteno-SiPc triads,<sup>27</sup> and this could favor exciplex formation with the Pc Q state. The longer carotenoid could also have a stronger charge-transfer character of the  $S_1$  state and promote further charge shift to Pc and exciplex formation; a carbonyl group in the carotenoid moiety of the dyads confers a partial charge-transfer character to the  $S_1$  state.<sup>28</sup>

It should be noted that the Pc Q bleach signals in the EADS of Figure 4A are made up of two components. These negative signals arise from both the population (and decay) of the Pc excited singlet state due to energy transfer from the carotenoid and from the exciplex formation, which depletes the ground state of Pc as well. The picosecond time scale decay of the bleach, the exciplex decay, correlates with the relaxation of the carotenoid  $S_1/S^*$  state. Because only ground-state Pc molecules are involved in the exciplex formation, the picosecond time scale decay of the Pc Q bleach does not constitute an additional decay pathway of the Pc excited state initially formed by energy transfer in dyad **3**.

**Dyad 1.** The results from a global analysis of the data for dyad **1** are shown in Figure 6A. Figures 6B–D show kinetic traces at selected wavelengths for dyad **1**. Six components are needed for a satisfactory fit of the data. The first EADS (black line) appears at time zero and represents population of the optically allowed  $S_2$  state of the carotenoid. It presents a region of negative signal below 570 nm originating from the carotenoid ground-state bleach and stimulated emission and a band-shift-like signal in the Pc Q region around 680 nm. It evolves in 37 fs into the second EADS (red line), which is characterized by ESA in the 480–600 nm region. The second EADS is assigned to a mixture of the vibrationally hot  $S_1$  state and the  $S^*$  state. The hot  $S_1$  ESA is expected to have a maximum around 560 nm while that of the  $S^*$  state is around 525 nm.

The second EADS also displays strong bleach at 680 nm corresponding to the Pc Q state and a dip at 610 nm that originates from a vibronic band of the Pc Q state superimposed on the ESA of both the Pc and the carotenoid moieties. The presence of the bleach in the Pc ground-state absorption region indicates that the carotenoid  $S_2$  state is active in transferring energy to Pc. The evolution to the third EADS (green line) takes place in 500 fs. It corresponds to a decrease of ESA at the red side of the  $S_1$  absorption, which may be assigned to vibrational cooling of the  $S_1$  state.<sup>29,30</sup> Moreover, an increase of the Pc Q bleach at 680 nm is observed that is likely to originate from energy transfer from the hot  $S_1$  state and possibly the  $S^*$  state to Pc. (Note that the third EADS overlaps with the fourth EADS,

**TABLE 2: Yields at Branching Points and Rate Constants for Dyad 3 in THF Obtained from Target Analysis**

$\Phi_1$	$\Phi_2$	$\Phi_3$	$\Phi_4$	$k_1$	$k_2$	$k_3$	$k_4$	$k_5$
30%	12%	34%	24%	$(1.4\text{ps})^{-1}$	$(102\text{ps})^{-1}$	$(5.7\text{ps})^{-1}$	$(18\text{ps})^{-1}$	$(750\text{ps})^{-1}$

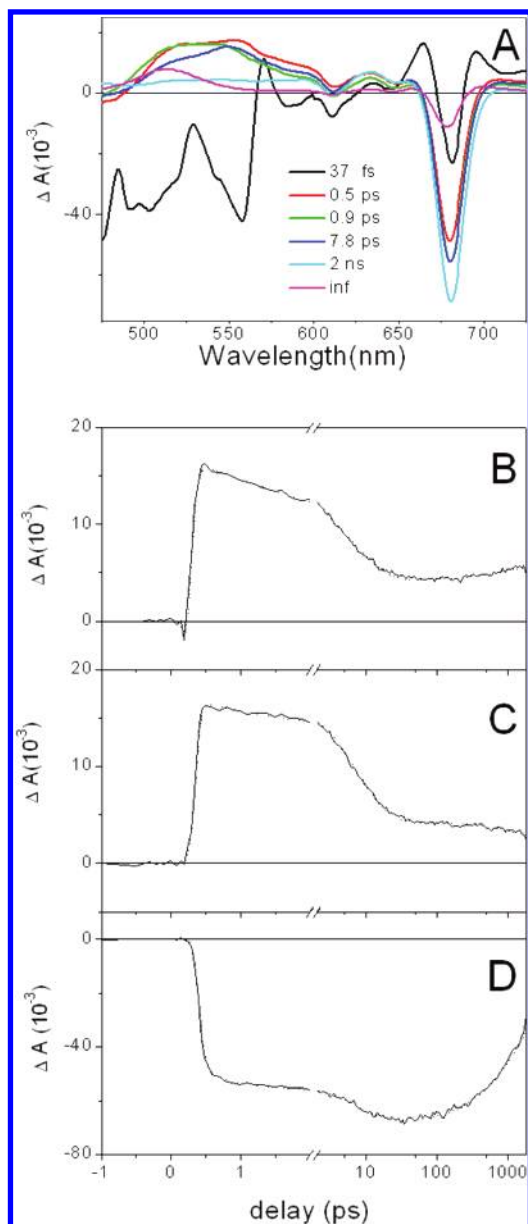


**Figure 6.** (A) Evolution-associated difference spectra that follow from a global analysis of data for dyad **1** in THF with excitation at 475 nm. (B) Kinetic trace with excitation at 475 nm and detection at 520 nm for dyad **1** (solid line), along with the result of the global analysis fit (dotted line). (C) Same as panel B with detection at 560 nm. (D) Same as panel B with detection at 680 nm.

blue line, in the Pc Q region and is not visible.) The next EADS (blue line) appears after 900 fs and has a lifetime of 7.8 ps. The signal in the 500–540 nm region, where the main contribution to the spectrum is given by  $S^*$ , has decreased, whereas the signal in the 540–620 nm region, where the absorption is mainly due to  $S_1$ , has slightly increased, indicating decay of  $S^*$  in about 0.9 ps, partly by IC to  $S_1$ , as observed for dyads **2** and **3** on similar time scales.

The evolution to the fifth EADS (cyan line) takes place in 7.8 ps. At this stage the carotenoid ESA has decayed, and the fifth EADS corresponds very well to that of the excited Pc Q state with a flat ESA in the 450–600 nm region.<sup>4</sup> Around 680 nm, the bleach presents a sizable increase with respect to the previous EADS, which implies that the carotenoid  $S_1$  state has transferred energy to Pc. Figure 6D shows the kinetic trace recorded at 680 nm corresponding to the maximum of the Pc Q absorption. The ultrafast rise of the bleach corresponding to

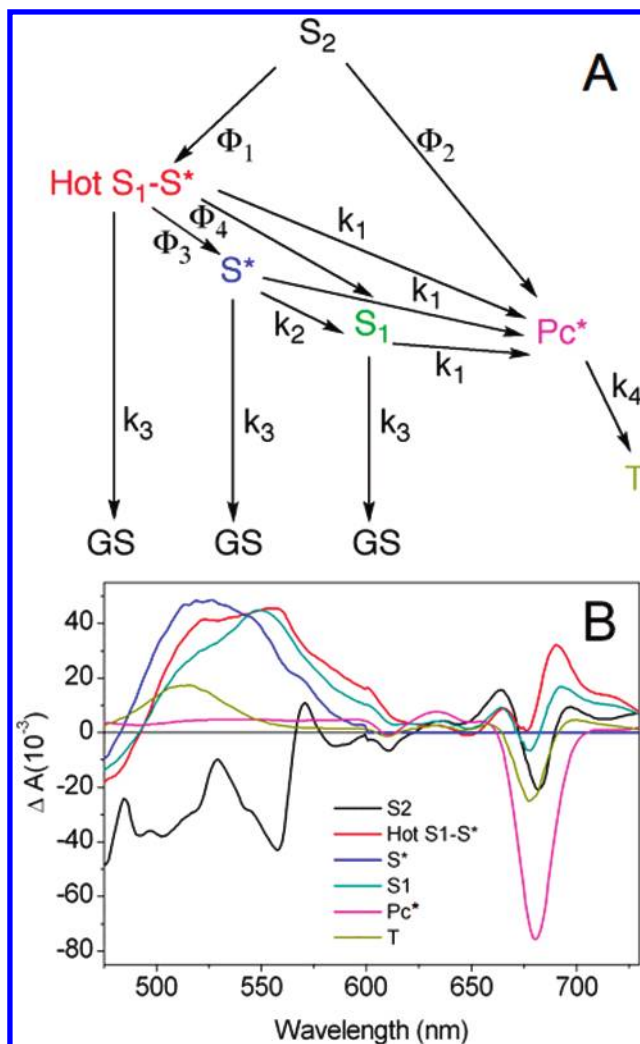


**Figure 7.** (A) Kinetic model used in the target analysis of the time-resolved data on dyad **1** (B) Species-associated difference spectra from the target analysis for dyad **1** in THF. See text for details.

the carotenoid  $S_2 \rightarrow Pc$  energy transfer is followed by two slower rises corresponding to hot  $S_1-S^* \rightarrow Pc$  and  $S_1 \rightarrow Pc$  energy transfer. The carotenoid to Pc energy transfer in dyad **1** is reminiscent of several natural light-harvesting antennas where high carotenoid to chlorophyll energy transfer efficiency is obtained by employing a multiphasic Car to Chl energy transfer.<sup>2,11,21,31–33</sup>

The final EADS (magenta line) appears after 2 ns and represents the component that does not decay on the time scale of the experiment. It features the typical carotenoid triplet ESA in the 475–550 nm region as well as a bleach/band-shift-like signal in the Pc Q region. Thus, the carotenoid triplet state rises directly upon decay of the singlet excited state of Pc. This observation implies that triplet–triplet energy transfer from Pc to the carotenoid occurs much faster than the ISC process in Pc, which effectively occurs in 2 ns. A similar phenomenon was observed recently in carotenoid-SiPc triads.<sup>16</sup>

**Target Analysis of Dyad 1.** To quantify the yields of the various energy transfer and energy deactivation pathways in dyad **1** we carried out a target analysis with the kinetic model depicted in Figure 7A.

The initially excited  $S_2$  state partly relaxes to the hot  $S_1-S^*$  state with a fraction  $\Phi_1$  and transfers energy to the phthalocyanine moiety (fraction  $\Phi_2$ ). From the hot  $S_1-S^*$  state the  $S^*$  and  $S_1$  states are populated in parallel with fractions  $\Phi_3$  and

**TABLE 3: Yields at Branching Points and Rate Constants for Dyad 1 in THF Obtained from Target Analysis**

$\Phi_1$	$\Phi_2$	$\Phi_3$	$\Phi_4$	$k_1$	$k_2$	$k_3$	$k_4$
31%	69%	70%	30%	(11 ps) <sup>-1</sup>	(1.1 ps) <sup>-1</sup>	(25 ps) <sup>-1</sup>	(1.98 ns) <sup>-1</sup>

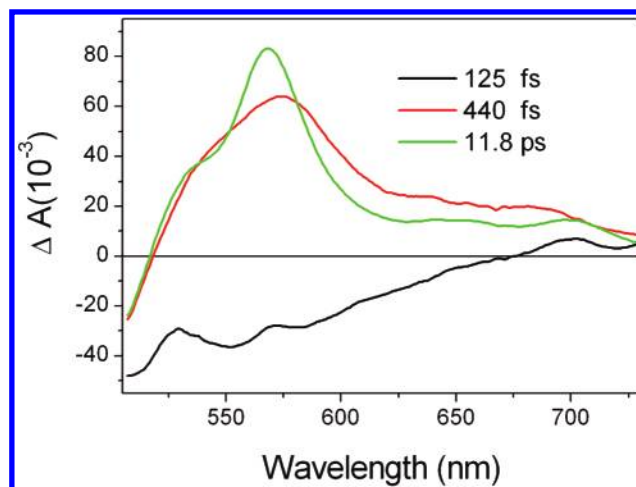
$\Phi_4$ , respectively. The hot  $S_1-S^*$  state relaxes to the ground state with a rate constant  $k_3$  and transfers energy to Pc with a rate constant  $k_1$ . The  $S^*$  state internally converts into the  $S_1$  state with a rate constant  $k_2$ , contributes to energy transfer to Pc with a rate constant  $k_1$ , and relaxes to the ground state with a rate constant  $k_3$ . The  $S_1$  state transfers energy to Pc with a rate constant  $k_1$  and relaxes to the ground state (rate constant  $k_3$ ). From the excited Pc a long-lived mixture of carotenoid and Pc triplets is populated with a rate constant  $k_4$ .

Figure 7B depicts the SADS obtained from the kinetic model while the fractions and rate constants are reported in Table 3. The black SADS corresponds to the initially excited carotenoid  $S_2$  state with a ground-state bleach below 560 nm. The hot  $S_1-S^*$  state (red SADS) shows a ground-state bleach below 500 nm and excited-state absorption associated with both the  $S^*$  and the  $S_1$  states. It relaxes in 0.5 ps (fixed in the analysis) to the  $S^*$  state (blue SADS) and  $S_1$  state (green SADS). The  $S^*$  state displays excited-state absorption blue-shifted with respect to  $S_1$  and a ground-state bleach below 490 nm. The  $S_1$  state displays the typical  $S_1 \rightarrow S_n$  excited-state absorption and a ground-state bleach below 500 nm. For both states the excited-state absorption regions are blue-shifted with respect to the hot  $S_1-S^*$  state.

The Pc excited state (magenta SADS) displays the Pc Q bleach at 677 nm and a vibronic band at 610 nm as well as a region of relatively flat excited-state absorption. The long-lived component shows the typical carotenoid  $T_1 \rightarrow T_n$  excited-state absorption in the 480–560 nm region and some residual Pc Q bleach meaning that the spectrum corresponds to a mixture of carotenoid and Pc triplet states.

**$S^* \rightarrow S_1$  Internal Conversion.** The experiments on dyad 2 indicate that upon excitation of the optically allowed carotenoid  $S_2$  state the  $S^*$  and  $S_1$  states are rapidly populated. Interestingly, the  $S^*$  state, besides relaxation to the ground state, undergoes IC to the  $S_1$  state. The similar evolution in the global analysis suggests that the same process is present in all three dyads. This is the first report of such an IC pathway in carotenoids and gives us more insight into the still mysterious nature of the  $S^*$  state. Showing that  $S^*$  can act as an intermediate state in the  $S_2 \rightarrow S_1$  IC pathway establishes unequivocally the singlet excited-state nature of the  $S^*$  state. Furthermore, the IC process allows us to locate  $S^*$  above  $S_1$  in these particular cases.

To investigate the role of the covalent linkage to Pc in the carotenoid excited-state dynamics, we performed a transient absorption measurement on carotenoid 2', a model for the carotenoid of dyad 2, where Pc has been replaced by a methyl ester. The results from a global analysis of the time-resolved data are shown in Figure 8. Three components are needed for a good fit of the data: the first spectrum (black line) appears at time zero and corresponds to carotenoid  $S_2$  state. It evolves into the second EADS (red line) in 125 fs. This spectrum has the typical shape of the hot  $S_1$  state and vibrationally relaxes in 440 fs.<sup>29,30</sup> The  $S_1$  state (green EADS) relaxes to the ground state in 11.8 ps. This evolution suggests that in the model carotenoid either the  $S^*$  state is not populated or it is not distinguishable from the  $S_1$  state; i.e., the two present the same dynamics. Thus, the presence of the covalently linked Pc in the dyad must be responsible for some specific interaction with the carotenoid leading to the separation of the  $S^*$  and  $S_1$  states

**Figure 8.** Evolution-associated difference spectra that follow from a global analysis of data for model carotenoid 2' in THF with excitation at 475 nm.**TABLE 4: Carotenoid to Phthalocyanine Energy Transfer Efficiency from the Various Excited States**

	dyad 1	dyad 2	dyad 3
$S_2$	69%	60%	24%
hot $S_1/S^*$ and $S^*$	<4%	0%	0%
$S_1$	20%	0%	0%

and to the ensuing IC process. Possibly, the presence of the covalently linked Pc leads to some distortion or twisting of the carotenoid, which could be responsible for the occurrence of the  $S^*$  state in the dyad and not in the model carotenoid. Interestingly, twisting or distortion of the carotenoid backbone has been shown to influence the properties of  $S^*$  in spirilloxanthin and spheroidene, where the extent of  $S^*$  formation and ultrafast triplet formation from the  $S^*$  state depends upon the degree of the deformation.<sup>11,13</sup>

The IC pathways available to  $S^*$  thus depend on how the carotenoid is bound in a specific system. In bacterial LH complexes and caroteno-SiPc triads,  $S^*$  and  $S_1$  evolve independently, which was explained by high energetic barriers between these states.<sup>9,16</sup> In the Car-Pc dyads studied herein,  $S^*$  rapidly internally converts to  $S_1$  on a sub-picosecond time scale, indicating a nearly barrierless transition. These observations indicate that in the various carotenoid-binding systems a large variation exists in the energy landscapes of the  $S^*$  and  $S_1$  potential energy surfaces. Very likely, these potential energy surfaces are strongly dependent on the exact geometry of the carotenoid and its specific interaction with nearby pigments. It is conceivable that  $S^*$  and  $S_1$  actually represent distinct local minima on the same potential energy surface and that it may not be appropriate to refer to them as separate electronic states.<sup>34</sup>

**Car to Pc Energy Transfer and Vice Versa.** Our study shows that the carotenoid to phthalocyanine energy transfer can be tuned by changing the conjugation length of the carotenoid. (For a summary of the results, see Table 4.) The efficiency of energy transfer to Pc from the optically allowed carotenoid  $S_2$  state is similar for dyads 1 and 2 and amounts to 69% and 60%, respectively. This number is significantly higher than that observed in caroteno-SiPc triads where the same carotenoids have been axially linked to the central silicon atom of Pc. In these systems, the energy transfer efficiency from the  $S_2$  state was found to be ~35%.<sup>16,35</sup> It is probable that the orientation of the transition dipole moments is more favorable for a dipole-coupling-based energy transfer mechanism in the dyads than in the triads, where the angle between the chromophores is close



to 90°. In addition a stronger electronic coupling by electron exchange terms is expected for the dyads, due to the partial conjugation provided by the amide bond, which is not present in the ester linkage of the caroteno-SiPc triads.

In dyad **1**, the carotenoid to Pc energy transfer is extremely efficient (>90%). Energy transfer from both the S<sub>2</sub> state and the optically forbidden, low-lying carotenoid state(s) is required to reach such a high efficiency. The addition of one double bond to the conjugation length of the carotenoid (dyad **2**) reduces the contribution from the low-lying S<sub>1</sub> state and leads to a drop in the energy transfer efficiency. It is likely that the carotenoid S<sub>1</sub> state energy, which is energetically above that of the Q state of Pc in dyad **1**, is lowered upon the extension of the conjugation length of the carotenoid so that the spectral overlap with the Pc Q state diminishes significantly. Indeed, in triads made up of the same carotenoids and a SiPc, the spectral overlap was estimated to diminish by a factor of 3 upon addition of one double bond to a 9 double-bond carotenoid.<sup>16</sup> This trend was corroborated by the study of the Pc Q state quenching in the same dyads reported herein where the addition of one double bond to the conjugation length, from dyad **1** to dyad **2**, turns the carotenoid S<sub>1</sub> state from an energy donor to the Pc Q excited state into a quencher of the Pc Q state.<sup>4</sup> This demonstrates the “molecular gear” mechanism in a model system, which has long been speculated to take place in plants.<sup>36,37</sup> Upon addition of another conjugated double bond to the carotenoid (dyad **3**), the S<sub>1</sub> state of the carotenoid becomes an even stronger quencher of the Pc Q excited state. Moreover, as described in this report for dyad **3**, the carotenoid excited state(s) appears to form an exciplex with the Pc ground state. This interaction could be fine-tuned by the local environment to lead to energy or electron transfer; experiments designed to test this and to look for similar states in natural systems are underway. Another factor possibly affecting the yield of S<sub>1</sub> energy transfer is the shorter intrinsic S<sub>1</sub> lifetime as the energy of the S<sub>1</sub> state is lowered. This IC follows roughly the energy gap law; typically, the S<sub>1</sub> lifetime of an 11 double-bond carotenoid is ~5 times shorter than that of a 9 double-bond carotenoid. It should be noted that the conjugated system of the carotenoid moiety in the dyads contains a carbonyl group, which confers a partial charge-transfer character to the S<sub>1</sub> state. This partial charge-transfer character has been shown to be responsible for the strong solvent polarity dependence of the Pc excited-state quenching by the carotenoid<sup>4</sup> and in principle could also affect the energy transfer efficiency from the S<sub>1</sub> state as was recently shown in similar systems.<sup>38</sup>

In contrast to many bacterial LH antennas and artificial caroteno-SiPc triads, the carotenoid S\* state does not transfer energy to Pc in dyad **2** or **3**. Given that in the former systems energy transfer from S\* occurred on the 5 ps to tens of picoseconds time scales, the absence of energy transfer from S\* in dyads **2** and **3** most likely follows from the fast (sub-picosecond) IC rates to S<sub>1</sub> and S<sub>0</sub>, which successfully compete with energy transfer.

LHCs of oxygenic photosynthetic organisms display trends in energy transfer characteristics similar to those observed here. In LHCII, CP43 and CP47 from plants and photosystem I (PSI) from cyanobacteria, the majority of excitations originating from carotenoids are transferred to Chl through the carotenoid S<sub>2</sub> state.<sup>21,32,39–41</sup> Energy transfer from the S<sub>1</sub> state was found to be dependent on the conjugation length of the carotenoid, with lutein and possibly neoxanthin being able to transfer efficiently from S<sub>1</sub>,<sup>21,32,42</sup> whereas β-carotene could only partly transfer from S<sub>1</sub> in PSI<sup>41,43</sup> and not at all in CP47, CP43, and the PSII reaction center.<sup>40,44</sup>

## Conclusions

By applying ultrafast time-resolved spectroscopy and rigorous spectro-temporal analysis, we have uncovered previously unobserved energy relaxation pathways and a novel type of collective carotenoid–phthalocyanine excited state in caroteno-phthalocyanine dyads. In dyads **1**, **2**, and **3**, which have a phthalocyanine covalently linked to a carotenoid with 9, 10, and 11 conjugated carbon–carbon double bonds, respectively, rapid internal conversion and energy transfer processes take place upon excitation of the carotenoid moiety at 475 nm. In all dyads we observed internal conversion from the optically allowed S<sub>2</sub> state to the optically forbidden S<sub>1</sub> and S\* states. Remarkably, internal conversion from S\* to S<sub>1</sub> occurs on a sub-picosecond time scale in all three dyads. This phenomenology contrasts with all previous observations of S\* in carotenoids and carotenoid-based LH systems, where S\* was found to evolve independently from all other carotenoid excited states.

In dyad **3**, we have characterized a novel type of collective carotenoid–phthalocyanine excited state, which we tentatively assign to a carotenoid–Pc exciplex. The exciplex is only observed in transient absorption upon excitation of the carotenoid and is non-emissive, and we therefore propose that it arises from population of the optically forbidden S\* and/or S<sub>1</sub> states, which excitonically couple with the Pc ground-state absorption through their strong S<sub>1</sub>/S\* → S<sub>n</sub> transition.

Finally, the results on dyads **1**, **2**, and **3** show that the carotenoid S<sub>2</sub> and S<sub>1</sub> energy levels must be matched to that of phthalocyanine for an optimal light-harvesting function. Dyad **1** exhibits a light-harvesting function at near unity through energy transfer from the optically allowed S<sub>2</sub> state and the optically forbidden S<sub>1</sub> state to phthalocyanine. In dyad **2**, efficient energy transfer from S<sub>2</sub> occurs, but energy transfer from S<sub>1</sub> is precluded, presumably as a result of unfavorable energetics. In dyad **3**, energy transfer efficiency from the 11 double-bond carotenoid to the phthalocyanine is low. The carotenoid S<sub>1</sub> state does not transfer energy, and the energy transfer quantum yield from S<sub>2</sub> is only ~24%. Remarkably, S\* does not appear to contribute significantly in the energy transfer process in any of the three dyads, which is likely related to its rapid internal conversion to the S<sub>1</sub> state.

The findings reported herein bear on the suggestion of a “molecular gear” mechanism controlling energy transfer between chlorophylls and carotenoids in plants.<sup>36,37</sup> While dyad **1** demonstrates S<sub>1</sub> to phthalocyanine energy transfer, in dyads **2** and **3** energy flows the other way — from the phthalocyanine to the carotenoid S<sub>1</sub>. The switch in energy flow with the change in conjugation length in a model system demonstrates the “molecular gear” mechanism in a model dyad system.

**Acknowledgment.** R.B. was supported by The Netherlands Organization for Scientific Research through the Earth and Life Sciences Council (NWO-ALW). J.T.M.K. was supported by NWO-ALW via a VIDI fellowship. The work was supported by the U. S. Department of Energy (Grant No. FG02-03ER15393). This is publication 673 from the ASU Center for the Study of Early Events in Photosynthesis.

**Supporting Information Available:** Selected spectroscopic data in different solvents, a set of kinetic traces, and time-gated spectra with fits obtained from the global analysis of the time-resolved data for the three dyads. This material is available free of charge via the Internet at <http://pubs.acs.org>.

## References and Notes

- (1) Frank, H. A.; Cogdell, R. J. *Photochem. Photobiol.* **1996**, *63*, 257.
- (2) Polivka, T.; Sundstrom, V. *Chem. Rev.* **2004**, *104*, 2021.

- (3) Holt, N. E.; Zigmantas, D.; Valkunas, L.; Li, X. P.; Niyogi, K. K.; Fleming, G. R. *Science* **2005**, *307*, 433.
- (4) Berera, R.; Herrero, C.; van Stokkum, I. H. M.; Vengris, M.; Kodis, G.; Palacios, R. E.; van Amerongen, H.; van Grondelle, R.; Gust, D.; Moore, T. A.; Moore, A. L.; Kennis, J. T. M. *Proc. Natl. Acad. Sci. U.S.A.* **2006**, *103*, 5343.
- (5) Tavan, P.; Schulten, K. *Phys. Rev. B* **1987**, *36*, 4337.
- (6) Hudson, B. S.; Kohler, B. E. *Chem. Phys. Lett.* **1972**, *14*, 299.
- (7) Starcke, J. H.; Wormit, M.; Schirmer, J.; Dreuw, A. *Chem. Phys.* **2006**, *329*, 39.
- (8) Sashima, T.; Nagae, H.; Kuki, M.; Koyama, Y. *Chem. Phys. Lett.* **1999**, *299*, 187.
- (9) Gradinaru, C. C.; Kennis, J. T. M.; Papagiannakis, E.; van Stokkum, I. H. M.; Cogdell, R. J.; Fleming, G. R.; Niederman, R. A.; van Grondelle, R. *Proc. Natl. Acad. Sci. U.S.A.* **2001**, *98*, 2364.
- (10) Cerullo, G.; Polli, D.; Lanzani, G.; De Silvestri, S.; Hashimoto, H.; Cogdell, R. J. *Science* **2002**, *298*, 2395.
- (11) Papagiannakis, E.; Kennis, J. T. M.; van Stokkum, I. H. M.; Cogdell, R. J.; van Grondelle, R. *Proc. Natl. Acad. Sci. U.S.A.* **2002**, *99*, 6017.
- (12) Larsen, D. S.; Papagiannakis, E.; van Stokkum, I. H. M.; Vengris, M.; Kennis, J. T. M.; van Grondelle, R. *Chem. Phys. Lett.* **2003**, *381*, 733.
- (13) Papagiannakis, E.; Das, S. K.; Gall, A.; van Stokkum, I. H. M.; Robert, B.; van Grondelle, R.; Frank, H. A.; Kennis, J. T. M. *J. Phys. Chem. B* **2003**, *107*, 5642.
- (14) Wohlleben, W.; Backup, T.; Herek, J. L.; Cogdell, R. J.; Motzkus, M. *Biophys. J.* **2003**, *85*, 442.
- (15) Billsten, H. H.; Pan, J. X.; Sinha, S.; Pascher, T.; Sundstrom, V.; Polivka, T. *J. Phys. Chem. A* **2005**, *109*, 6852.
- (16) Kodis, G.; Herrero, C.; Palacios, R.; Marino-Ochoa, E.; Gould, S.; de la Garza, L.; van Grondelle, R.; Gust, D.; Moore, T. A.; Moore, A. L.; Kennis, J. T. M. *J. Phys. Chem. B* **2004**, *108*, 414.
- (17) Papagiannakis, E.; van Stokkum, I. H. M.; Vengris, M.; Cogdell, R. J.; van Grondelle, R.; Larsen, D. S. *J. Phys. Chem. B* **2006**, *110*, 5727.
- (18) Wohlleben, W.; Backup, T.; Hashimoto, H.; Cogdell, R. J.; Herek, J. L.; Motzkus, M. *J. Phys. Chem. B* **2004**, *108*, 3320.
- (19) Gust, D.; Moore, T. A.; Moore, A. L. *Acc. Chem. Res.* **2001**, *34*, 40.
- (20) Berera, R.; Moore, G. F.; van Stokkum, I. H. M.; Kodis, G.; Liddell, P. A.; Gervaldo, M.; van Grondelle, R.; Kennis, J. T. M.; Gust, D.; Moore, T. A.; Moore, A. L. *Photochem. Photobiol. Sci.* **2006**, *5*, 1142.
- (21) Gradinaru, C. C.; van Stokkum, I. H. M.; Pascal, A. A.; van Grondelle, R.; van Amerongen, H. *J. Phys. Chem. B* **2000**, *104*, 9330.
- (22) van Stokkum, I. H. M.; Larsen, D. S.; van Grondelle, R. *Biochim. Biophys. Acta* **2004**, *1657*, 82.
- (23) Gradinaru, C. C.; van Grondelle, R.; van Amerongen, H. *J. Phys. Chem. B* **2003**, *107*, 3938.
- (24) Herek, J. L.; Wendling, M.; He, Z.; Polivka, T.; Garcia-Asua, G.; Cogdell, R. J.; Hunter, C. N.; van Grondelle, R.; Sundstrom, V.; Pullerits, T. *J. Phys. Chem. B* **2004**, *108*, 10398.
- (25) Polivka, T.; Zigmantas, D.; Sundström, V.; Formaggio, E.; Cinque, G.; Bassi, R. *Biochemistry* **2002**, *41*, 439.
- (26) Birks, J. B. *Rep. Prog. Phys.* **1975**, *38*, 903.
- (27) Palacios, R. E.; Kodis, G.; Herrero, C.; Ochoa, E. M.; Gervaldo, M.; Gould, S. L.; Kennis, J. T. M.; Gust, D.; Moore, T. A.; Moore, A. L. *J. Phys. Chem. B* **2006**, *110*, 25411.
- (28) Zigmantas, D.; Hiller, R. G.; Sharples, F. P.; Frank, H. A.; Sundstrom, V.; Polivka, T. *Phys. Chem. Chem. Phys.* **2004**, *6*, 3009.
- (29) Billsten, H. H.; Zigmantas, D.; Sundström, V.; Polivka, T. *Chem. Phys. Lett.* **2002**, *355*, 465.
- (30) de Weerd, F. L.; van Stokkum, I. H. M.; van Grondelle, R. *Chem. Phys. Lett.* **2002**, *354*, 38.
- (31) Zigmantas, D.; Hiller, R. G.; Sundström, V.; Polivka, T. *Proc. Natl. Acad. Sci. U.S.A.* **2002**, *99*, 16760.
- (32) Croce, R.; Muller, M. G.; Bassi, R.; Holzwarth, A. R. *Biophys. J.* **2001**, *80*, 901.
- (33) Zhang, J. P.; Fujii, R.; Qian, P.; Inaba, T.; Mizoguchi, T.; Koyama, Y.; Onaka, K.; Watanabe, Y.; Nagae, H. *J. Phys. Chem. B* **2000**, *104*, 3683.
- (34) Niedzwiedzki, D. M.; Sullivan, J. O.; Polivka, T.; Birge, R. R.; Frank, H. A. *J. Phys. Chem. B* **2006**, *110*, 22872.
- (35) Marino-Ochoa, E.; Palacios, R.; Kodis, G.; Macpherson, A. N.; Gillbro, T.; Gust, D.; Moore, T. A.; Moore, A. L. *Photochem. Photobiol.* **2002**, *76*, 116.
- (36) Frank, H. A.; Cua, A.; Chynwat, V.; Young, A.; Gosztola, D.; Wasielewski, M. R. *Photosynth. Res.* **1994**, *41*, 389.
- (37) Frank, H. A.; Cua, A.; Chynwat, V.; Young, A.; Gosztola, D.; Wasielewski, M. R. *Biochim. Biophys. Acta* **1996**, *243*.
- (38) Polivka, T.; Pellnor, M.; Melo, E.; Pascher, T.; Sundstrom, V.; Osuka, A.; Naqvi, K. R. *J. Phys. Chem. C* **2007**, *111*, 467.
- (39) Holt, N. E.; Kennis, J. T. M.; Dall'Osto, L.; Bassi, R.; Fleming, G. R. *Chem. Phys. Lett.* **2003**, *379*, 305.
- (40) Holt, N. E.; Kennis, J. T. M.; Fleming, G. R. *J. Phys. Chem. B* **2004**, *108*, 19029.
- (41) de Weerd, F. L.; Kennis, J. T. M.; Dekker, J. P.; van Grondelle, R. *J. Phys. Chem. B* **2003**, *107*, 5995.
- (42) Walla, P. J.; Yom, J.; Krueger, B. P.; Fleming, G. R. *J. Phys. Chem. B* **2000**, *104*, 4799.
- (43) Wehling, A.; Walla, P. J. *J. Phys. Chem. B* **2005**, *109*, 24510.
- (44) de Weerd, F. L.; Dekker, J. P.; van Grondelle, R. *J. Phys. Chem. B* **2003**, *107*, 6214.